Microporous and Mesoporous Materials 144 (2011) 19–27

Contents lists available at ScienceDirect

Microporous and Mesoporous Materials

journal homepage: www.elsevier.com/locate/micromeso

Zeolite films and membranes. Emerging applications ☆

M.P. Pina, R. Mallada, M. Arruebo, M. Urbiztondo, N. Navascués, O. de la Iglesia, J. Santamaria *

Nanoscience Institute of Aragon, University of Zaragoza, 50 009 Zaragoza, Spain

ARTICLE INFO

Article history:
Received 10 September 2010
Received in revised form 26 November 2010
Accepted 1 December 2010
Available online 13 December 2010

Keywords:
Zeolite film
Microreactor
Membrane
Sensor

ABSTRACT

Zeolite films can be grown, either as individual crystals or as intergrown layers on a wide variety of supports including metal surfaces, ceramic and polymeric plates, metallic wires, organic and inorganic fibers and even surfaces with especial characteristics, such as electronic circuits or medical prostheses. These zeolite films constitute a special type of nanostructured interface capable of very specific interactions with individual molecules. Because of this, in many cases it is possible to implement molecular recognition functions, in addition to exploiting other well known zeolite properties such as their catalytic, adsorption and diffusion/permeation characteristics. This overview discusses some of the emerging possibilities of zeolite films, with an emphasis on applications at the microscale.

1. Introduction

Although most zeolite users still think of zeolites as powdered materials, in fact zeolites can be grown as films on a variety of supports, both inorganic (e.g. glass, ceramic, metal) and organic (e.g. plastics, cellulose, wood). This allows the transfer of some of the characteristic properties of zeolites (such as adsorption, catalysis, molecular recognition and diffusion) to a 2-dimensional structure, with potential applications in areas ranging from reactor engineering to molecular separations and chemical analysis.

During the last two decades considerable progress has been achieved in controlling the growth of zeolite films of a varied nature, as described in a number of recent reviews [1–6]. In many cases, the objective is to obtain a zeolite membrane for gas or liquid phase separations. This application requires excellent intergrowth between the zeolite crystals that make up the membrane, to minimize the number of inter-crystalline gaps that are considered as membrane defects because of their highly negative impact on the separation selectivity. At the opposite end are zeolite coatings, in which the zeolite layer consists of individual crystals, which are attached to the support by physical or chemical bonds. In this case crystal intergrowth is not sought and may even be undesirable, when the final application is a zeolite-coated sensor or a zeolite catalytic coating on a microreactor channel [7]. Therefore, the characteristics of zeolite films can be very different depending on the intended application, and the preparation procedures have to be tailored accordingly. This overview does not intend to repeat what is already described in the previously cited reviews. Instead it discusses recent developments in the field of zeolite films for three main areas of application: zeolite membranes for separations and delivery of molecules, zeolite coatings for catalytic microreactors and zeolite-based gas sensors. This work focuses on films consisting of zeolite only, and therefore the many examples of zeolite-containing composites are explicitly excluded from this overview.

2. Zeolite membranes for separation, controlled permeation and other applications

Solvent dehydration remains to date the only industrial application of zeolite membranes. Mitsui Engineering and Shipbuilding Co. pioneered the field in 2000, and together with its subsidiary BNRI has about 100 pervaporation units in operation [8]. Other companies (including GmBH-HITK in Germany, ECN in the Netherlands, Kühni in Switzerland and Hitachi Zosen in Japan) have followed suit and now offer their own zeolite-based pervaporation or vapor permeation dehydration systems. However, in spite of the excellent performance shown by zeolite membranes in many laboratory studies of gas and liquid phase separations there are no other commercial applications of zeolite membranes. The reasons for this are varied, with membrane cost (estimated in 2004 to be in excess of US$3000/m^2 of membrane [9]) at their forefront. Although most of this cost (around 70% [10]) can be attributed to the cost of the ceramic supports commonly used for zeolite membranes, the lack of suitable alternatives makes them at least one order of magnitude more expensive than their polymeric counterparts. Even for the star application of zeolite membranes,

☆ Keynote lecture presented at the 16th International Zeolite Conference (16th IZC), jointly organised with the 7th International Mesostructured Materials Symposium (7th IMMS), held in Sorrento, Italy, July 4–9, 2010.

* Corresponding author. Fax: +34 976762142.
E-mail address: Jesus.Santamaria@unizar.es (J. Santamaria).

1387-1811/$ - see front matter © 2010 Elsevier Inc. All rights reserved.
doi:10.1016/j.micromeso.2010.12.003

dehydration of organic solvents, Van-Hoof et al. [11] showed that if pervaporation is only used to break the azeotrope, polymeric membranes are preferred, and only when pervaporation is used to dehydrate to very low water concentration the zeolite membranes are to be considered. Another problem that still hinders industrial application of zeolite membranes relates to their relatively poor reproducibility [8]. This is due to the intrinsic complexity of a preparation process that involves critical stages such as seeding, hydrothermal synthesis with sufficient/continuous supply of reactants and also in most cases removal of the structure-directing agent by calcination. However, reproducibility is essential for mass production, and additional investigations to quantify and improve membrane reproducibility are needed [12].

The disadvantages currently associated to zeolite membranes (mainly their high cost and complex fabrication procedure) imply that their use in separations will likely be restricted to those scenarios where the unique properties of zeolites (thermal and chemical stability, shape selective separation) come into play [10]. Indeed, high-selectivity separations are possible with zeolite membranes. However, especially for gas phase separations, this requires nearly perfect membranes, with a very low concentration of defects: the separation selectivity plummets as the number of defects (inter-crystalline gaps a few nanometers in size) increases. Caro and coworkers [13] recently discussed the difficulties in preparing shape-selective Al-rich zeolite membranes. They pointed to two main reasons: the negative surface charge of the growing membrane, that makes difficult for negatively charged silica species in the solution to approach and close up inter-crystalline gaps, and the mismatch in the expansion coefficient between the zeolite membrane and the metal or ceramic support. The first problem was tackled in a subsequent work of the same group [14], where a cationic polymer was used to provide positive charge to the membrane support, facilitating the capture of negatively charged LTA nutrients and thus leading to improved membranes. As for the difference in expansion coefficients between the membrane and the support, it becomes critical when drying the membrane after synthesis or when calcining the membranes to remove the structure-directing agent, which, even if carried out at very low heating rates, gives rise to mechanical stress that results in crystal boundary defects and cracks that impair membrane performance. Recently, Tsapatsis and coworkers [15] proposed a novel procedure termed rapid thermal processing (RTP) to reduce boundary defect formation by strengthening bonding at the crystal boundaries. These authors hypothesized that since RTP involves high heating rates (ca. 700 K/min) condensation of Si-OH groups between adjacent crystal grains occurs, leading to grain bonding before tensile stress builds up. Indeed, the RTP treated membranes showed a reduced concentration of defects under fluorescent confocal microscopy, and a correspondingly enhanced permeation selectivity.

For large-scale application of zeolite membranes, in addition to permeation selectivity the membranes must also provide a sufficiently high permeation flux. These two requirements are frequently in conflict: highly selective membranes are often thick membranes (since the probability of intercrystalline defects running across the membrane thickness decreases as the membrane becomes thicker), while the permeability is inversely proportional to membrane thickness. In spite of this, thin (1 μm or less) zeolite membranes with good gas phase selectivity already exist (see [16,17] as recent examples). As an alternative, high flux can also be obtained in thick membranes (ca. 30 μm) by manipulating the synthesis process in order to create an additional non-zeolite pore system. Richter et al. [18] achieved this for MFI membranes by replacing part of the water in the synthesis gel with alcohol, obtaining a strong increase in permeation fluxes with a modest decrease in selectivity.

While the process of scaling up zeolite membranes is affected by the problems discussed such as cost or development of intercrystalline defects, the same problems are alleviated in scaled-down systems [2]. Thus for instance, the cost of a sub-mm size zeolite film would represent only a small fraction of the total cost of a smart electronic-nose sensor system and therefore ceases to be an issue for this type of application. At the same time, the probability of obtaining a defect-free membrane increases as its surface decreases, and the small size also helps in relieving the mechanical stress generated during thermal treatments. Finally, for small-scale systems, self-supported zeolite membranes can be contemplated, avoiding the pressure drop and the costs associated to the porous inorganic supports that are commonly used. All of this has paved the way to a new generation of systems and devices that use zeolite layers with a relatively small size in a variety of roles. Some of these are schematised in Fig. 1.

In 2003, Chau et al. [19] successfully demonstrated selective gas permeation in zeolite micromembranes. This miniaturization allows improving mass and heat transfer rates and enable the design of more efficient, safer and compact separation units. Potential applications include separations for the pharmaceutical and fine chemical industry, lab-on-a-chip devices, rapid adsorption-screening tools and micro fuel cells. The same group showed that zeolite micro fuel cells could achieve a performance comparable to Nafion®-based PEMFCs [20] and that self-supported micromembranes prepared on silicon supports were able of good selectivities and permeation fluxes [21,22]. Self-supported silicalite micromembranes were also prepared in our laboratory on laser-perforated stainless steel sheets [23]. Avoiding the mass transfer resistance of a porous support resulted in permselective separations at much higher fluxes than those on supported MFI membranes. Stainless-steel-net-imbedded ZSM-5 [24] and silicalite-1 [25] membranes, have also shown excellent selectivities for heavy metal removal and CO_2 separations, respectively. Recent advances following these miniaturization approaches have been described elsewhere [26].

There are also many applications of zeolite films that are not aimed towards separations and therefore do not require permselectivity. This is for instance the case of zeolite films acting as diffusion barriers or as porous reservoirs from which the controlled release of a given molecule can be obtained. We have proposed the use of zeolitic micromembranes as diffusion controlling barriers on drug-eluting hollow implants used in traumatology and in orthopedic surgery [27]. In this approach the inner volume of the hollow implant is loaded with a drug (e.g. an antibiotic to prevent bacterial biofilm formation on the surface of the implant). Burst release of the drug is avoided by using a zeolitic micromembrane as a window on the implant through which sustained drug release can be achieved since the hollow volume of the implant is used as a large drug reservoir. Fig. 2 shows an example of iodine (~0.27 nm) release through the zeolite micropores (~0.55 nm). With the same system the permeation of methylene blue (~0.7 × 1.6 nm) could not be detected, which points to a very low concentration of intercrystalline defects, as could be expected for a self-supported membrane, where the absence of support means that the expansion coefficient mismatch and the corresponding stresses during calcination are largely avoided. In addition to membrane-capped reservoirs, drug delivery can also be contemplated from nanoporous coatings (zeolite, ordered mesoporous silica) on medical devices [28]. The ordered porous structure of zeolite coatings becomes especially useful for controlled drug delivery when the zeolite pore size approaches the hydrodynamic diameter of the enclosed drug, since in this case drug diffusion kinetics follow linear non-Fickian behavior approaching zero-order release [29].

An even more desirable scenario would be to have permeation controlled by an external physical or chemical stimulus. Some

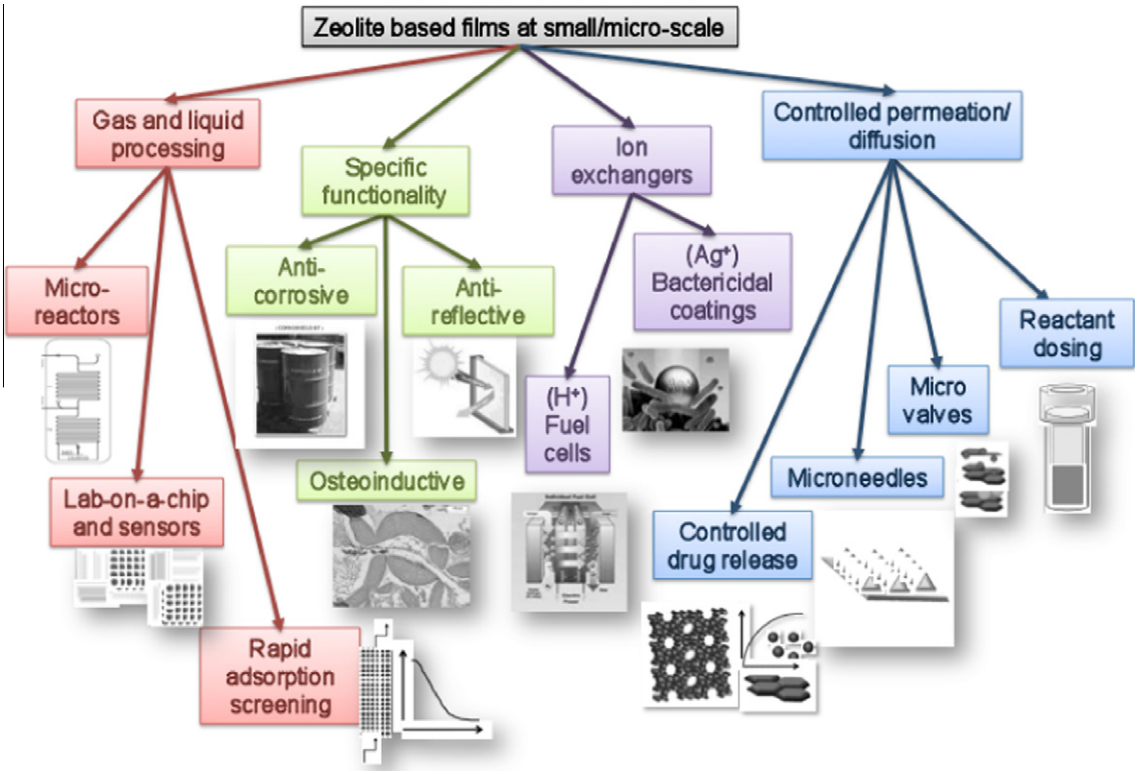

Fig. 1. Some emerging applications of zeolite films at the microscale.

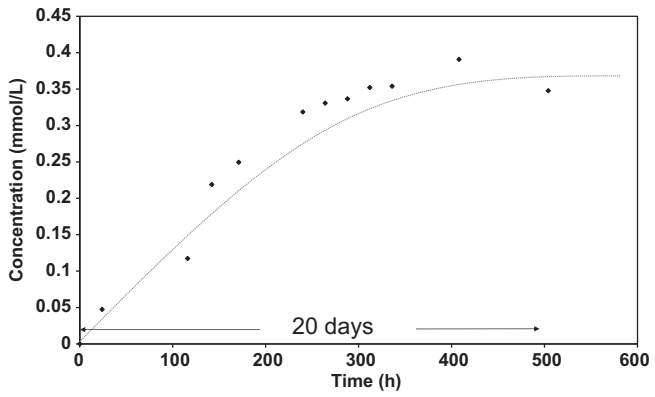

Fig. 2. An example of the use of zeolite membranes for controlled drug delivery. Release of iodine from a reservoir in which a 1 mm diameter pinhole was capped with a silicalite micromembrane prepared by using 4 successive hydrothermal syntheses in order to minimize intercrystalline defects. The iodine molecule (~0.27 nm) was able to diffuse through the zeolite micropores (~0.55 nm) but not the methylene blue (~0.7 × 1.6 nm) which remained below the detection limit, using UV–VIS spectrophotometry, during the time tested.

steps have already been taken in this direction. Thus, Weh et al. [30] demonstrated photo-switchable modification of gas permeation through a zeolite membrane by adsorbing azobenzene on the zeolite pore walls. Azobenzene undergoes cis–trans photo isomerization leading to an increased permeance in the trans-state. Potential applications of this technology includes light-controlled drug delivery, reactant dosing and product removal. Other chemical systems for light-controlled gating of zeolite pores have also been proposed [31].

Another field of application for zeolite-based drug delivery is the release of Ag^+ ions from silver-exchanged zeolite coatings. Silver cations are effective against bacteria (even at low loadings in the zeolite [32]), viruses, and some eukaryotic microorganisms, and therefore silver-exchanged zeolites are nowadays used on medical and surgical equipment including endotracheal tubes, dental filling materials, medical dressings, bandages, surgical meshes and catheters. Silver-exchanged zeolites have also been used to confer antimicrobial properties to Portland cement mortars, food packaging, ointments, stainless steel, paper, paints, and plastic products. An example of a silver-releasing zeolite coating from our laboratory can be seen in Fig. 3.

Not only silver, but also other components have been loaded within the open framework of zeolites for applications in medicine and biology. In this way, Wheatley et al. [33] adsorbed nitric oxide, which is considered an antianginal drug and causes vasodilatation on zeolites and again this approach has been extrapolated to coatings to be used on medical devices by the same authors [34]. The protective capabilities of the zeolite pores to protect hosted molecules from degradation (thermal, chemical, biochemical or mechanical) have also been exploited to encapsulate dyes [35], Gd^{3+} ions (to avoid the toxicity of free Gd ions in gastrointestinal contrast agents used in MRI applications), amino acids [36], and so on. These capabilities can be easily extrapolated to coatings and films.

Zeolite structures can also be used for drug delivery without using the zeolite pores for storage. This is the case of microneedles made of zeolite, whose use has been proposed for transdermal drug delivery systems [37]. The authors claim that by virtue of their small dimensions and their ability to penetrate into skin tissue in a non-invasive manner the risk for infection is minimized and the microneedles provide a painless injection.

Finally, zeolite-based films are increasingly being used as anticorrosive coatings: studies have been carried out on aluminium-based alloys and on stainless steel under acidic and alkaline conditions [38] and in concrete sewers to protect them from biologically generated sulphuric acid [39]. Corrosion-resistant zeolite coatings have been reported for biomedical implants [40], with the

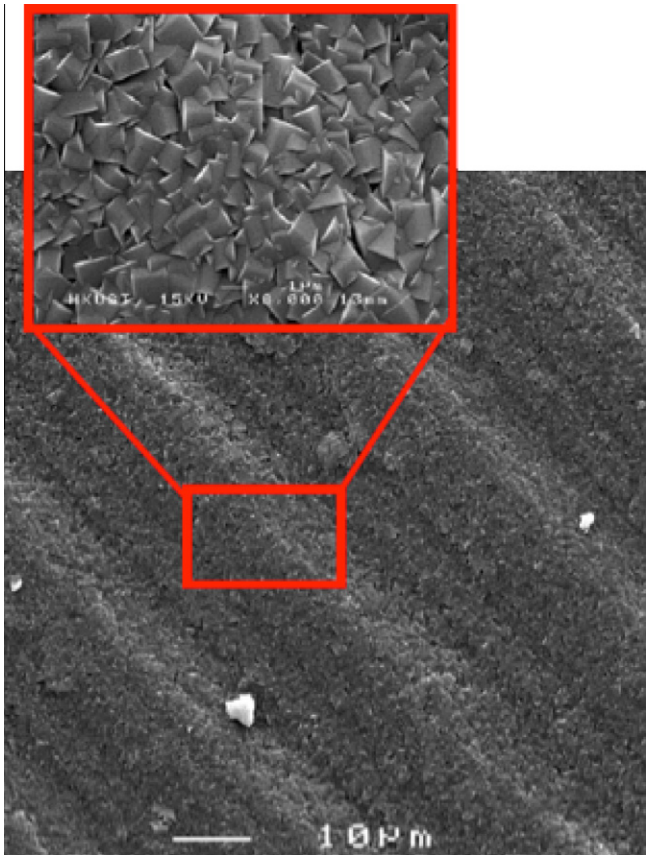

Fig. 3. A silver-loaded MFI zeolite coating grown on a polymer disk, to be used as part of a medical prosthesis for in-situ delivery of bactericidal Ag^+ ions.

added advantage of being able to promote proliferation of human fetal osteoblast cells when applied on titanium alloys [41]. Other less common applications of zeolite films include hydrophilic coatings for improved heat transfer [42] as well as anti-reflective coatings [43].

3. Zeolite coatings for catalytic microreactors

The start of microreaction technology can be traced to the emphasis on process miniaturization and process intensification in the 1990s [44,45] but the field has continued to expand at a brisk pace, driven by the obvious advantages of microreaction technology that include enhanced mass and heat transfer, safer operation and easy scale-up by replica.

However, microreaction engineering still has to face many remaining problems, and one of the most pressing relates to the development of methods to deposit a sufficient amount of catalyst in the microdevice. Packing a powdered catalyst in the reactor microchannels presents obvious difficulties in terms of pressure drop and flow distribution and therefore the solutions have generally aimed towards the deposition of thin catalytic coatings on the reactor wall [46]. These coatings should not only provide enough catalytic load, but also be able do this in a homogeneous way, with high mechanical stability and good accessibility of the reactants to the catalyst (high external surface/volume ratio in the coating). Ideally, the catalyst would be an integral part of the microreactor.

In most instances, catalytic coatings on microreactors consist of a catalyst-containing layer washcoated on the reactor wall. However, for the cases in which the catalyst is supported on zeolites or is a zeolite itself, a zeolite film directly grown on the microreactor channels appears as the ideal candidate: it yields a highly adherent catalytic layer, a binder is not needed (meaning that the layer is 100% catalyst) and the considerable experience gathered in the synthesis of zeolite films allows to regulate film thickness and crystal orientation.

Rebrov et al. [47] carried out the pioneering investigations of zeolite growth in stainless steel microchannels studying the effect gel composition, time, temperature, orientation of the support and number of synthesis, for ZSM-5 films on 500 µm wide microchannels. A two-step hydrothermal synthesis was used, with a first synthesis providing "in-situ seeding", and a second synthesis for seed growth into crystals. The resulting zeolite layer was ion exchanged with Ce and tested in the selective reduction of NOx using ammonia as reducing agent, with the microreactor catalytic film clearly outperforming the pelletized catalysts. The same group devised a system for scaling-up the hydrothermal synthesis of ZSM-5 on molybdenum plates by designing a special procedure that allowed a total of 72 plates to be processed simultaneously by hydrothermal synthesis [48]. A coverage close to 15 g/m^2 was obtained with very good homogeneity.

In collaboration with IMM, we have also studied the preparation of MFI layers on microchannels by three different synthesis methods: hydrothermal synthesis, seeded hydrothermal synthesis and steam assisted crystallization [49]. The seeded hydrothermal method, with a careful control of gel dilution and temperature, was adequate for controlling the thickness of the zeolite layer, resulting in well-intergrown zeolite coatings on the channel surface. On the other hand, the steam assisted crystallization method allowed a better control of the location of the zeolite film, avoiding deposition in the interchannel space. It also provided a better accessibility to the catalyst by maintaining the individuality of the zeolite crystals. However, the synthesis time to obtain a zeolite layer was between 8 and 16 days. The ZSM-5 microreactors were ion-exchanged with Pt and tested in the selective oxidation of CO, SELOX reaction [50], where complete CO conversion was achieved at 170 °C.

In addition to MFI, zeolites such as MOR [51–53], ETS-10 [52], BEA [54], LTA [55] and FAU [52,56], have also been prepared as catalytic layers on different supports such as ceramic monoliths, brass, molybdenum and stainless steel microchannel reactors. In the case of MOR and ETS-10 [52], the seeded hydrothermal growth procedure was tailored to obtain films where the growth of individual crystals, rather than crystal intergrowth was the dominant feature, thus improving catalyst accessibility (Fig. 4). The zeolite layers and the ion exchange procedure were shown to be reproducible and the adherence of the catalyst was excellent, with well over 90% of the zeolite layer remaining after a harsh ultrasonication treatment. The FAU and ETS-10 coated microreactors exhibited high performance in the selective oxidation of CO in a simulated reformer stream with total CO combustion temperatures as low as 125 °C [57]. Other reactions investigated include a wide variety of systems ranging from ammoxidation of ethylene [54] to combustion of VOCs at trace concentration levels [56] and Knovenagel condensation [58].

The Yeung group has developed several strategies for the preparation of zeolite layers onto microchemical systems and microchannels etched on silicon wafers [59,60], ranging from the simple deposition of zeolite powder in the microchannel to methods involving hydrothermal synthesis, which on a Si wafer presents significant difficulties of its own, related to chemical attack to the support under the highly alkaline synthesis conditions. In a different approach [60] a uniform zeolite layer was grown on the silicon wafer and then patterned in a variety of shapes using photolithography etching processes adapted from those employed in the semiconductor industry. The same authors [61,62] went on to coat 5 µm thick TS-1 zeolite layers on microchannels 33 mm long, 500 µm wide, fabricated onto silicon wafers. Different

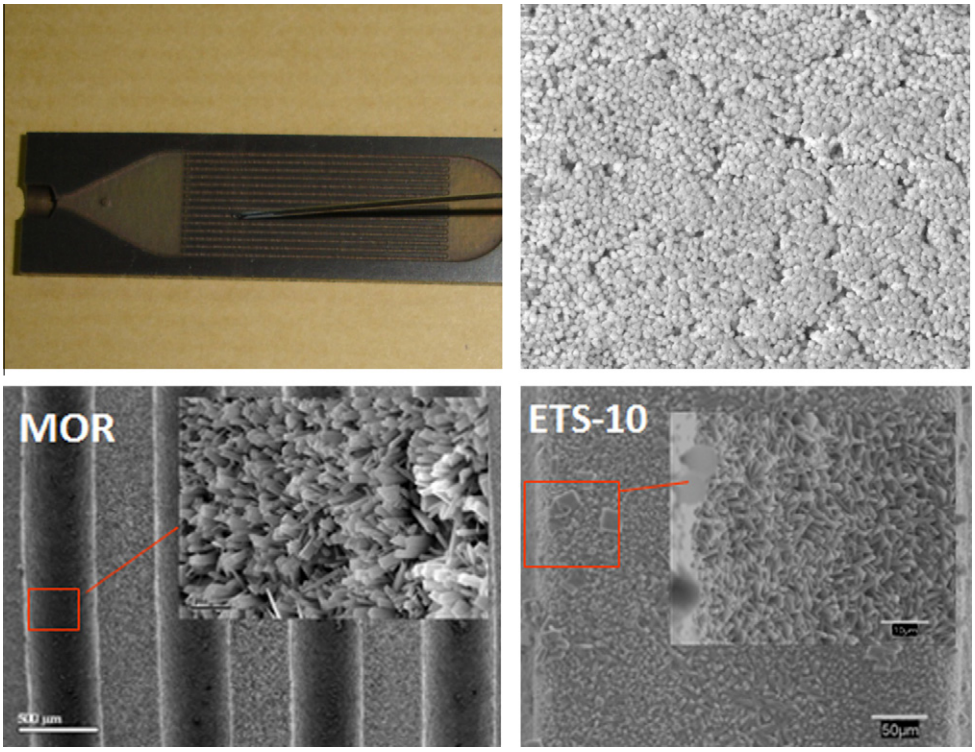

Fig. 4. Zeolite layers on microreactor channels. (a) Depositing a seed suspension on the microreactor channels. (b) View of the channel surface after the seeding procedure. (c and d) Views of the channel surface after hydrothermal synthesis of MOR and ETS10 layers.

configurations of the microreactors (single channel, T-shaped and multichannel microreactor) were used for the epoxidation of 1-pentene.

Finally, photolithography processes were also used to prepare zeolite-coated microreactors with ultrahigh external surface to volume ratios [63]. To this end, regular structures of SiO_2 micromonoliths and microneedles (Fig. 5) with a diameter of 3–5 μm were created on silicon wafers by photoassisted electrochemical etching and covered with a uniform zeolite layer using seeded hydrothermal synthesis. The thin zeolite coating (<1 μm) provided a short diffusion path length, and the external area of the zeolite films was 400,000–750,000 $m^2/m^3$of reactor volume, underlying the potential of these microstructures as highly efficient contactors.

4. Zeolite-based gas sensors

The sensitivity of gas sensors has improved dramatically over the last decade. Femtogram detection limits are almost routinely achieved with present day nanoelectromechanical devices (NEMS) and the most advanced devices are now approaching zeptogram (10^{-21} g) [64] level resolution. This dramatic improvement has been due to advances in three areas: smaller mechanical resonators, higher resonant frequencies and improved readout techniques to detect the motion. Regarding sensor selectivity, (i.e. the ability to respond only, or at least predominantly, to certain components in a mixture, and not to others), comparable advances have not been achieved. Sensing a specific gas phase analyte in a mixture where other components may interfere still remains a significant challenge. However, achieving sufficient selectivity is critical in many applications, such as in the case of the so-called electronic noses [65], increasingly demanded multisensor arrays in the fields of food, cosmetic and pharmaceutical industry, security, environmental monitoring and clinical diagnostics.

In view of the molecular recognition properties that nanoporous solids can afford, it is not surprising that they have been employed as selectivity enhancers on already existing high-sensitivity platforms. Zeolites are obvious candidates for this role, in view of their

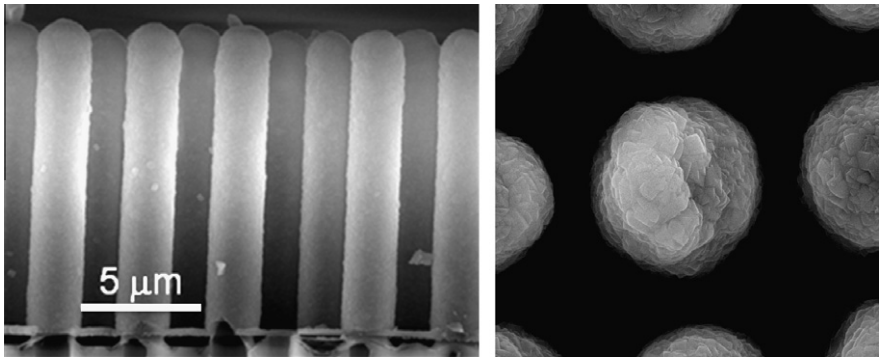

Fig. 5. SEM (side view) of a zeolite-coated microneedle array. Right: detail of the zeolite-coated needles (top view).

well-defined porous structure and their tunable adsorption properties and ion-exchange capacity, as pointed out in recent reviews [66–68]. Next, we describe different sensor concepts involving zeolites as individual crystals or as intergrown films, according to the type of transducer used.

4.1. Zeolites as hosts for active species in optical sensors

A typical optical chemical sensor employs an analyte-sensitive species, whose optical properties vary in the presence of the molecule to be detected. The main problem with these sensors is often related to the photo-instability, meaning decomposition or evaporation on extended exposure to light [69]. Avoiding this problem is difficult since the sensor response depends on exciting the sample. Moreover, as many of the sensors are designed for use in fiber optic systems, the sensor mass is small and a relatively low number of molecules must handle the intense light exposures necessary for adequate signal-to-noise ratio. In this case zeolites come into play on account of their high thermal and mechanical stability as well as their optical transparency in the visible region and fast response towards ultraviolet radiation [70,71]. The porous structure of the zeolites allows the encapsulation of organic chromophores, providing a protective environment that increases their stability. In addition, the incorporation of optically active guest molecules in crystallographically defined positions or highly organised arrangements often result in peculiar host–guest interactions which can be exploited for sensing. The composition, morphology and pore size of the zeolite can be optimized for the sensing of specific analytes (e.g. O_2 [72,73], VOCs [74,75], humidity [74,76]). Thus for instance, the encapsulation of Nile red inside the pores of commercial zeolite Y has been used for continuous water and hexane detection by deploying the Nile Red-FAU composite coating on a standard plastic optical fiber [75]. The dye-FAU composite coating exhibited improved properties in terms of water sensitivity, response time and chromophore stability.

4.2. Zeolite films as selective barriers for interfering species

The deployment of zeolite films on sensor platforms has mainly been attempted for conventional n-or p-type semiconducting sensor materials. The zeolite framework structure, Si/Al ratio, extra-framework cations and thickness of the film are the main parameters for a fine-tuning of the barrier effect. The first sensor platform incorporating a set of four MOS with layers of different zeolites dates back to 1986 [77]. A decade later, Fukui and Nishida [78] used commercial crystals of FAU and FER zeolites with colloidal silica as binder to cover the sensing layer of La_2O_3-Au/SnO_2 sensors, and were able to eliminate ethanol interference during CO sensing. Different zeolite masks, also consisting of commercial crystals, have been used to minimize the interference of O_2 in YSZ NO_2 sensors [79]. Mann and coworkers [80] applied Cr-FAU and Cr-BEA coatings onto $Cr_{2-x}Ti_xO_y$ sensors to discriminate a series of alkanes. Recently, FAU overlayers onto WO_3 or $Cr_{2-x}Ti_xO_y$ sensors [81] have been deployed to increase ethanol against carbon monoxide response. In these works the zeolite coatings produce a variety of adsorption, catalytic and diffusive effects, that become useful to enhance or depress the sensor response towards a given analyte, often on an ad hoc basis. Catalytic effects have been explicitly exploited to remove interfering components, often through combustion reactions. An example is the work of Sahner et al. [82,83] who used screen-printed thick films of the $SrTi_{1-x}Fe_xO_{3-\delta}$ perovskite (a p-type semiconductor) with an additional top layer of Pt/ZSM5 to remove the interference of CO in the sensing of NO. In this system the gases passed through the Pt/ZSM5 coating where the combustion of CO took place prior to reaching the sensor itself.

In contrast to the above works, that used powdered zeolites as sensor overlayers, other investigations have addressed intergrown zeolite films that can play an even more discriminating role as a reactive or non-reactive barrier [84]. In previous works of our laboratory [85,86] MFI and LTA membranes were directly synthesized on screen-printed Pd/SnO_2 sensor layers. These molecular filters decreased interference of undesired molecules mainly via a selective adsorption mechanism that hindered the diffusion of less strongly adsorbed species. Depending on the operating conditions used, the cross-sensitivity of the zeolite-modified sensors towards certain analytes could be significantly reduced, and in some cases suppressed altogether, thus strongly increasing the sensing selectivity. In a subsequent work [87] the system was scaled down by a factor of 50, and a microdropping procedure was used to deposit the zeolite barrier (see Fig. 6). The micromachined sensor presented a considerable reduction of response times without apparent loss of performance. Using a similar concept the sensor sensitivity and response time for selective ethylene gas detection were improved using b-oriented silicalite-1 layers prepared by hydrothermal synthesis onto SnO_2 thin film sensors [88]. The silicalite layer was able to preferentially adsorb the non-polar analyte (ethylene) blocking the path of water and producing a sensor with less moisture interference. At the same time, the b orientation of the film favored diffusion, thus reducing sensor response time.

4.3. Zeolites as ion conductors and catalysts in solid state gas sensors

Zeolites exhibit intrinsic conductivity [89] and can play the role of ion conductors. In particular, by ion exchange, ionic-liquid encapsulation or functionalization procedures, the proton conductivity of hydrated microporous materials can be strongly increased, opening their application in high temperature Proton Exchange Membrane (PEM) fuel cells [89]. Besides, as mobile cations present within the zeolite framework may hop from one binding site to the next, dehydrated zeolites exhibit ionic conductivity with activation energies ranging from 40 to 100 kJ/kmol [90]. This enables the

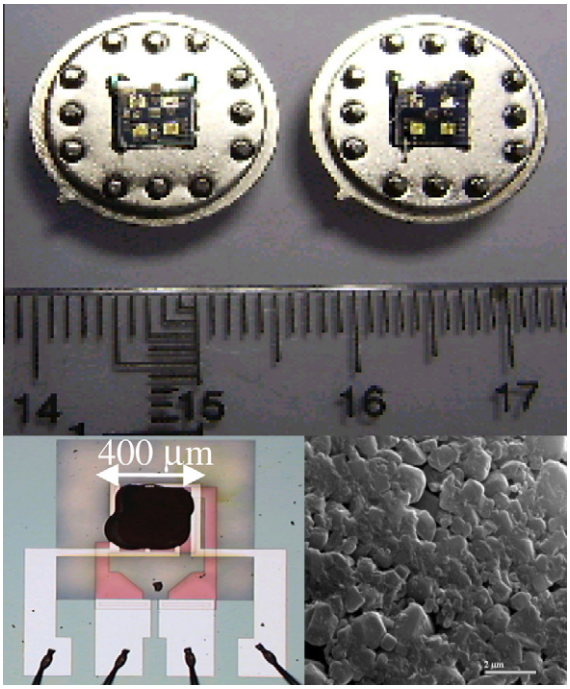

Fig. 6. Top: two microfabricated sensors, each containing 4 zeolite-coated units. Bottom: Left: one of the zeolite-coated Pd/SnO_2 sensors. Right: SEM view of the zeolite coating.

design of sensors based on changes that take place on the ionic conductivity through interactions with gas phase species.

Schäf et al. [91] were the first to propose a conductometric sensor with zeolites, using natural phillipsite and stilbite crystals attached to Au electrodes for detection of humidity and alcohols. In this case the presence of water molecules causes a sterical hindrance for cationic motion and therefore the conduction process is influenced by the presence of gas molecules capable of accessing the zeolite channel system [92]. Following the same concept, in our laboratory [93] different zeolite coatings have been deployed on top of Interdigital Capacitive Structures (IDC) working at room temperature. In this field the extensive work carried out by the Moos group is noteworthy, especially regarding the sensing of exhaust gases, ammonia and hydrocarbons with a variety of zeolite-modified sensors (conductimetric, potentiometric and impedimetric) [94–104]. Also very interesting is the impedance-based sensor developed by Dutta et al. [105] for detection of dimethylmethylphosphonate (DMMP), a molecule representative of toxic nerve agents. In this case, the presence of DMMP at ppm levels, could be detected by the increase of the ionic conductivity of the Na-Y zeolite due to the binding of the sodium cation with the phosphonate group of DMMP. The zeolite-modified sensors can be extremely robust, as shown by the impedimetric H-ZSM-5 based humidity sensor capable of working under harsh conditions (reducing atmosphere (H_2) and temperature up to 600° C) and still provide a linear and reversible response [106].

4.4. Zeolites in resonant sensors

Piezoelectric sensor devices (quartz crystal microbalances, QCMs) work on the principle of measuring small changes in the resonant frequency of an oscillating piezoelectric crystal due to changes in the mass on the sensor surface. Since any mass deposited on the QCM would give rise to a change in frequency, some procedure is needed to guarantee that the variation observed corresponds to the desired chemical species and not to other gas phase analytes. The molecular sieving and selective surface interactions provided by different zeolites has made them candidates as analyte targets in this type of sensors (as an example in the patent literature see [107]). Zeolite-modified QCMs have been employed to detect ethanol (using MFI zeolite [108]), humidity (using LTA and BEA zeolites [109]), and NO, SO_2, and water (using LTA, silicalite-1, and sodalite [110,111]). In our laboratory [112] hydrophilic ($AlPO_4$-18) and hydrophobic (silicalite-1) layers were deployed on QCM sensors for propane and humidity sensing (see Fig. 7). The different coatings substantially eliminated the interference of the complementary species (i.e. the silicalite sensor showed a strong sensitivity for propane and almost null for water, when sensed in the presence of propane, while the opposite was true for the $AlPO_4$-18 loaded sensor).

Another interesting platform are the so-called magneto-elastic sensors, whose low material and operational costs allow for their use on a disposable basis [113,114]. Briefly, magnetoelastic

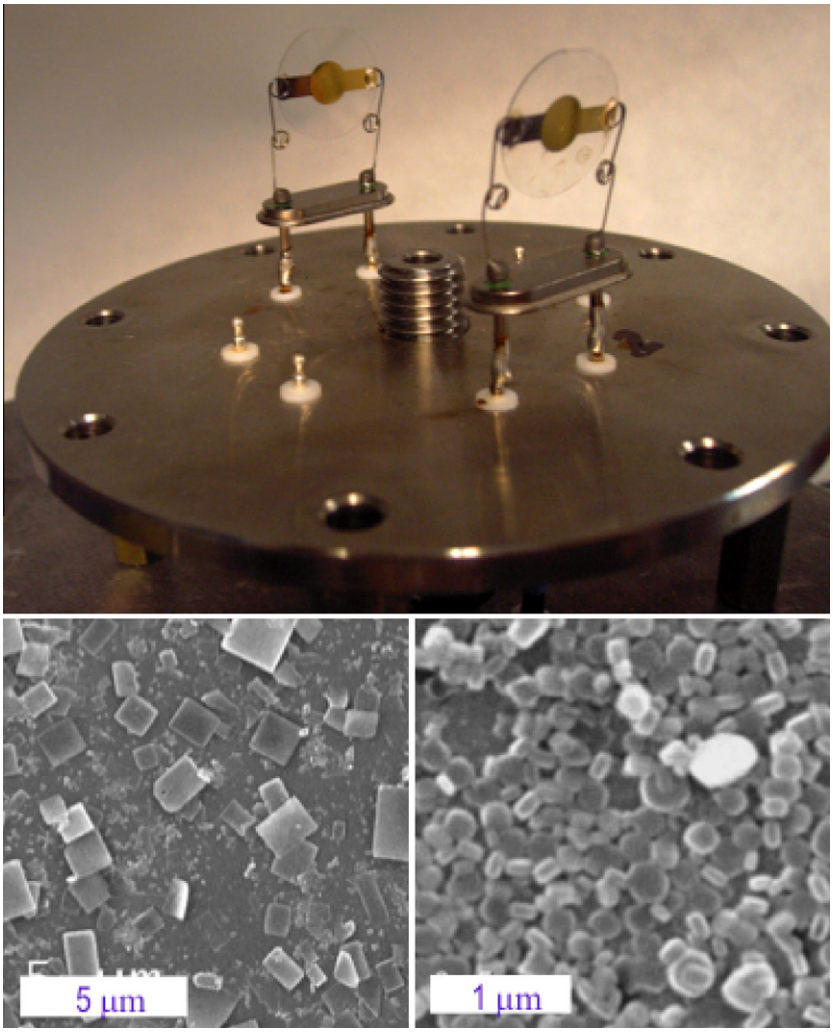

Fig. 7. Top: part of a gas sensing unit showing 2 zeolite-coated QCMs. Bottom: SEM views of the $AlPO_4$-18 and SIL coatings, respectively.

materials are usually amorphous metallic alloys, commonly known as Metglas, or composites of rare-earth elements, such as Terfenol which can be set to resonate under an external alternating magnetic field, generating both acoustic and magnetic fluxes which can be detected. The most frequently used material is Metglas 2826 MB ($Fe_{40}N_{38}Mo_4B_{18}$) magnetoelastic ribbon (Allied Signal). Similarly to QCMs, a shift in the resonant frequency occurs when the sensor is alternately exposed to air and to the analyte gas. The preparation of FAU and b-oriented silicalite layers onto Metglas supports and their performance as sensors have been recently reported for the detection of *n*-C_4 and iso-C_4 and CO_2, respectively [115,116]. Again, the zeolite is used here to impart selectivity to the sensor: the zeolite–Metglas composites combine the ability of zeolite to selectively adsorb hydrocarbons with the ability of the Metglas alloy to convert mass loads and changes in elastic properties to measurable shifts in the sensor's resonance frequency.

Similarly to QCMs, cantilever-based sensors can also be configured to work as tiny microbalances in which the analysis of changes in the resonance frequency (dynamic mode) or in the deflection (static mode) of the cantilever can be used to determine mass loadings with extremely high sensitivity, as already noted. The selectivity problem becomes even more critical here, since the high sensitivity sought means that minute amounts of other species are able to interfere with the measurement. In spite of this, the coupling of zeolites and cantilevers has scarcely been explored. The seminal investigation here corresponds to Scandella et al. [117], who exploited the *lab on a tip* concept proposed in their previous work [118] and demonstrated water detection in the nanogram range by attaching a few ZSM-5 crystals to a silicon cantilever. More recently, Zhou and coworkers [119,120] deposited a drop of a dilute suspension containing zeolite MFI crystals on a cantilever, and then used it to sense Freon, and Wakayama and coworkers [121] developed hybrid ceramic/Si cantilevers and then glued some crystals of an unspecified zeolite type to the cantilever to carry out some basic sensing of water vapor. In our laboratory [122] we have developed preparation methods for zeolite-modified cantilevers, including the design of the cantilever itself and the methods to obtain reproducible zeolite coatings of a varied nature. The new generation of cantilevers will have an optimized geometry to maximize sensor response locally as well as integrated heating of the zeolite layer to provide quick absorption–desorption cycle (see Fig. 8 as an example of a paddle-shaped cantilever to maximize the zeolite load). By tailoring the Si/Al ratio of the zeolite film and by introducing appropriate exchange cations it is possible to specifically increase the sensor sensitivity towards a given analyte (e.g. the detection of *o*-nitrotoluene at concentrations under 1 ppm by introduction of Co in BEA zeolite [122]).

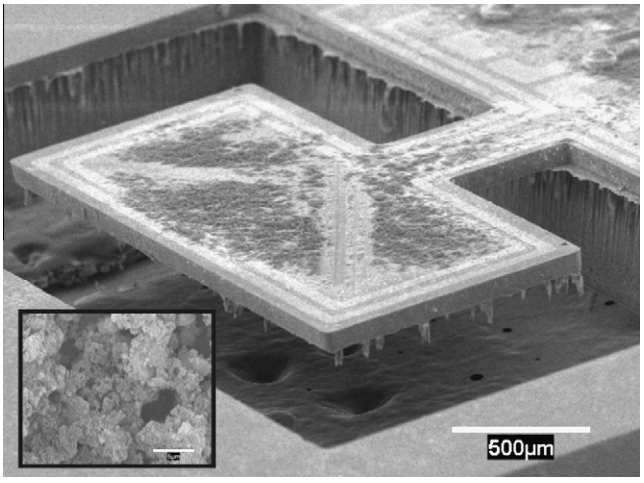

Fig. 8. SEM view of paddle-shaped Si cantilevers modified by Co-BEA zeolite nanocrystals: (insert: detail of the zeolite coating).

The cantilevers just discussed consist of a zeolite layer on top of a silicon cantilever. In this case the Si cantilever is the resonant element, and the zeolite layer on top of it acts as a target for the objective molecules. It is obvious that in this case most of the cantilever mass (the silicon support) is not sensitive towards the gas phase molecules. Given the experience gained in the patterning of zeolite films through wet and dry etching methods [60,123], the fabrication of self-supported zeolite structures becomes possible, opening the way towards zeolite-only cantilevers [124].

5. Conclusions

The experience gained in recent years allows the production of zeolite films on almost any type of support, with unprecedented control on their morphology, orientation and degree of crystal intergrowth. In spite of this, the only industrial application of zeolite membranes (solvent dehydration) is already a decade old, and new industrial-scale developments are not foreseen for the near future. Instead, a number of small-scale applications are emerging (in micromembranes, in drug delivery devices, in microreactors and in chemical sensors to name 4 areas of intense activity) that seem highly promising. These applications make full use of the intrinsic characteristics of zeolites. However given their small size the main problems that plague large scale applications (such as cost and presence of grain boundary defects) are no longer forbidding issues.

References

[1] J. Coronas, J. Santamaria, Top. Catal. 29 (2004) 29–44.
[2] J. Coronas, J. Santamaria, Chem. Eng. Sci. 59 (2004) 4789–4885.
[3] E.E. McLeary, J.C. Jansen, F. Kapteijn, Microp. Mesop. Mater. 90 (2006) 198–220.
[4] J. Caro, M. Noack, Microp. Mesop. Mater. 115 (2008) 215–233.
[5] Y.S. Li, W.S. Yang, J. Membr. Sci. 316 (2008) 3–17.
[6] M. Zhou, B.Q. Zhang, X.F. Liu, Chin. Sci. Bull. 53 (2008) 801–816.
[7] M. Arruebo, R. Mallada, J. Santamaria, in: J. Cejka, J. Peréz-Pariente, W. J. Roth (Eds.), Zeolites: From Model Materials to Industrial Catalysts, Transworld Research Network, Trivandrum, 2008, pp. 125–250.
[8] S.L. Wee, C.T. Tye, S. Bhatia, Sep. Purif. Technol. 63 (2008) 500–516.
[9] R.W. Baker. Membrane Technology and Applications. Second ed., Ed. John Wiley & Sons Ltd., 2004, pp. 314.
[10] J. Caro, M. Noack, P. Kölsch, Adsorpt.-J. Int. Adsorpt. Soc. 11 (2005) 215–227.
[11] V. Van-Hoof, C. Dotremont, A. Buekenhoudt, Sep. Purif. Tech. 48 (2006) 304–309.
[12] Navajas A., Mallada R., Téllez C., Coronas J., Menéndez M., Santamaria J., J. Membr. Sci., 299, (2007), 166–173.
[13] J. Caro, D. Albrecht, M. Noack, Sep. Purif. Tech. 66 (2009) 143–147.
[14] A. Huang, J. Caro, Chem. Mater. 22 (2010) 4353–4355.
[15] J. Choi, H.K. Jeong, M.A. Snyder, J.A. Stoeger, R.I. Masel, M. Tsapatsis, Science 325 (2009) 590–593.
[16] L. Sandstrom, M. Palomino, J. Hedlund, J. Membr. Sci. 254 (2010) 171–177.
[17] J.C. White, P.K. Dutta, K. Shqau, H. Verweij, Langmuir 26 (2010) 10287–10293.
[18] H. Richter, H. Vob, I. Voigt, A. Diefenbacher, G. Schuch, F. Steinbach, J. Caro, Sep. Purif. Tech. 72 (2010) 388–394.
[19] J.L.H. Chau, A.Y.L. Leung, K.L. Yeung, Lab Chip 3 (2003) 53–55.
[20] S.M. Kwan, K.L. Yeung, Chem. Commun. (2008) 3631–3633.
[21] Y.L.A. Leung, K.L. Yeung, Chem. Eng. Sci. 59 (2004) 4809–4817.
[22] S.M. Kwan, Y.L.A. Leung, K.L. Yeung, Sep. Purif. Tech. 73 (2010) 44–50.
[23] E. Mateo, R. Lahoz, G. de la Fuente, A. Paniagua, J. Coronas, J. Santamaría, Chem. Mater. 16 (2004) 4847–4850.
[24] X. Zou, G. Zhu, H. Guo, X. Jing, D. Xu, X. Qiu, Microp. Mesop. Mater. 124 (2009) 70.
[25] H. Guo, G. Zhu, H. Li, X. Zou, X. Yin, W. Yang, S. Qiu, R. Xu, Angew. Chem. Int. Ed. 45 (2006) 7053.
[26] M.A. Snyder, M. Tsapatsis, Angew. Chem. Int. Ed. 46 (2007) 7560.
[27] Arruebo M., Irusta, Pérez L.M., Lalueza P., Puértolas J.S., Gracia L., García-Álvarez F.E., Monzón M., Santamaría J., Spanish patent application, (2009) P200931157.
[28] M. Arruebo, N. Villaboa, J. Santamaría, Expert Opin. Drug Deliv. 7 (2010) 1–15.
[29] F. Martin, R. Walczak, A. Boiarski, M. Cohen, T. West, C. Cosentino, J. Shapiro, M. Ferrari, J. Control. Release 102 (2005) 123–133.

[30] K. Weh, M. Noack, K. Hoffmann, K.P. Schroder, J. Caro, Microp. Mesop. Mater. 54 (2002) 15–26.
[31] M. Fujiwara, T. Kitabayashi, K. Shiokawa, T.K. Moriuchi, Chem. Eng. J. 146 (2009) 520.
[32] P. Lalueza, M. Monzón, M. Arruebo, J. Santamaría, Chem. Commun. 47 (2011) 680–682.
[33] P.S. Wheatley, A.R. Butler, M.S. Crane, S. Fox, B. Xiao, A.G. Rossi, I.L. Megson, R.E. Morris, J. Am. Chem. Soc. 128 (2006) 502–509.
[34] Morris R.E., Wheatley P.S., Butler, A.R., WO2005003032 (A1) patent. Date: 2005-01-13.
[35] K.J. Balkus, A.A. Welch, B.E. Gnade, J. Inclusion Phenom. Macrocyclic Chem. 10 (1991) 141–151.
[36] J.E. Krohn, M. Tsapatsis, Langmuir 22 (2006) 9350–9356.
[37] Yeung K.L., Wong L., Sun W., et al. Patent Number(s): WO2007095859-A1; US2007280878-A1; CN101389374-A. (2007).
[38] A. Mitra, Z. Wang, T. Cao, H. Wang, L. Huang, Y. Yan, J. Electrochem. Soc. 149 (2002) B472–B478.
[39] T. Haile, H. Nakhla, Geomicrob. J. 25 (2008) 322–331.
[40] R.S. Bedi, D.E. Beving, L.P. Zanello, Y.S. Yan, Acta Biomater. 5 (2009) 3265–3271.
[41] R.S. Bedi, L.P. Zanello, Y.S. Yan, Adv. Funct. Mater. 19 (2009) 3856–3861.
[42] R.A. Munoz, D. Beving, Y.S. Yan, Ind. Eng. Chem. Res. 44 (2005) 4310–4315.
[43] G. Shu, J. Liu, A.S.T. Chiang, R.W. Thompson, Adv. Mater. 18 (2006) 185–189.
[44] P.L. Mills, D.J. Quiram, J.F. Ryley, Chem. Eng. Sci. 62 (2007) 6992–7010.
[45] J.J. Lerou, K.M. Ng, Chem. Eng. Sci. 51 (1996) 1595–1614.
[46] E.V. Rebrov, A. Berenguer-Murcia, A.E.H. Wheatley, B.F.G. Johnson, J.C. Schouten, Chim. Oggi-Chem. Today 27 (2009) 4–7.
[47] E.V. Rebrov, G.B.F. Seijger, H.P.A. Calis, M.H.J.M. de Croon, C.M. van den Bleek, J.C. Schouten, Appl. Catal. A: Gen. 206 (2001) 125–143.
[48] M.J.M. Mies, J.L.P. van den Bosch, E.V. Rebrov, J.C. Jansen, M.H.J.M. de Croon, J.C. Schouten, Catal. Today 110 (2005) 38–46.
[49] O. de la Iglesia, V. Sebastián, R. Mallada, G. Nikolaidis, J. Coronas, G. Kolb, R. Zapf, V. Hessel, J. Santamaría, Catal. Today 125 (2007) 2–10.
[50] G. Kolb, V. Hessel, V. Cominos, C. Hofmann, H. Löwe, G. Nikolaidis, R. Zapf, A. Ziogas, E.R. Delsman, M.H.J.M. de Croon, J.C. Schouten, O. de la Iglesia, R. Mallada, J. Santamaria, Catal. Today 120 (2007) 2–20.
[51] M.A. Ulla, R. Mallada, J. Coronas, L. Gutierrez, E. Miró, Chem. Commun. 5 (2004) 528–529.
[52] V. Sebastián, O. de la Iglesia, R. Mallada, L. Casado, G. Kolb, V. Hessel, J. Santamaría, Microporous Mesoporous Mat. 115 (2008) 147–155.
[53] J.M. Zamaro, E. Miró, Catal. Commun. 10 (2009) 1574–1576.
[54] M.J.M. Mies, E.V. Rebrov, J.C. Jansen, M.H.J.M. de Croon, J.C. Schouten, J. Catal. 247 (2007) 328–338.
[55] G. Yang, X. Zhang, S. Liu, K.L. Yeung, J. Wang, J. Phys. Chem. Solids 68 (2007) 26–31.
[56] N. Navascués, M. Escuin, Y. Rodas, S. Irusta, R. Mallada, J. Santamaría, Ind. Eng. Chem. Res. 49 (2010) 6941–6947.
[57] V. Sebastian, S. Irusta, R. Mallada, J. Santamaría, Catal. Today, 147 S1 (2009) S10.
[58] W.N. Lau, K.L. Yeung, X.F. Zhang, R. Martin-Aranda, Stud. Surf. Sci. Catal. 170 (2007) 1460–1465.
[59] Y.S.S. Wan, J.L.H. Chau, A. Gavriilidis, K.L. Yeung, Microporous Mesoporous Mat. 42 (2001) 157–175.
[60] J.L.H. Chau, Y.S.S. Wan, A. Gavriilidis, K.L. Yeung, Chem. Eng. J. 88 (2002) 187–200.
[61] Y.S.S. Wan, J.L.H. Chau, K.L. Yeung, A. Gavriilidis, J. Catal. 223 (2004) 241–249.
[62] W.T. Wong, Y.S.S. Wan, K.L. Yeung, A. Gavriilidis, Stud. Surf. Sci. Catal. 158 (2005) 2081–2088.
[63] M.A. Urbiztondo, E. Valera, T. Trifonov, R. Alcubilla, S. Irusta, M.P. Pina, A. Rodríguez, J. Santamaría, J. Catal. 250 (2007) 190–194.
[64] Y.T. Yang, C. Callegari, X.L. Feng, K.L. Ekinci, M.L. Roukes, Nano Lett. 6 (2006) 583–586.
[65] T.C. Pearce, S.S. Schiffman, H.T. Nagle, J.W. Gardner (Eds.), Handbook of Machine Olfaction: Electronic Nose Technology, Willey-VCH Verlag GmbH & Co. KGaA, Weinheim, 2003.
[66] M.A. Urbitzondo, M.P. Pina, J. Santamaría, in "Ordered Porous Solids", Valtchev, V. and Mintova S. (Eds.), Elsevier, 2009, pp. 381–405
[67] X. Xu, J. Wang, Y. Long, Sensors 6 (2006) 1751–1764.
[68] K. Sahner, G. Hagen, D. Schonauer, S. Reiß, R. Moos, Solid State Ionics 179 (2008) 2416–2423.
[69] J.N. Demas, B.A. DeGraff, Coord. Chem. Rev. 211 (2001) 317–351.
[70] G. Schulz-Ekloff, D. Wöhrle, B. Duffel, R.A. Schoonheydt, Microporous Mesoporous Mater. 51 (2002) 91–138.
[71] G. Calzaferri, S. Huber, H. Maas, C. Minkowski, Angew. Chem. 42 (2003) 3732–3758.
[72] B. Meier, T. Werner, I. Klimant, O.S. Wolfbeis, Sens. Actuators, B: Chem. 29 (1995) 240–245.
[73] K. McGilvray, M. Chretien, M. Lukeman, J. Scaiano, Chem. Commun. 42 (2006) 4401–4403.
[74] J. Meinershagen, T. Bein, J. Am. Chem. Soc. 121 (1999) 448–449.
[75] I. Pellejero, M. Urbiztondo, D. Izquierdo, S. Irusta, I. Salinas I, M.P. Pina, Ind. Eng. Chem. Res. 46 (2007) 2335–2341.
[76] S. Sohrabnezhad, A. Pourahmad, M. Sadjadi, Mater. Lett. 61 (2007) 2311–2314.
[77] R. Müller, E. Lange, Sens. Actuators 9 (1986) 39–48.
[78] K. Fukui, S. Nishida, Sens. Actuators, B: Chem. 45 (1997) 101–106.
[79] N.F. Szabo, H. Du, S.A. Akbar, A. Soliman, P.K. Dutta, Sens. Actuators, B 82 (2002) 142–149.
[80] D.P. Mann, T. Paraskeva, K.F.E. Pratt, I.P. Parkin, D.E. Williams, Meas. Sci. Technol. 16 (2005) 1193–1200.
[81] R. Binions, H. Davies, A. Afonja, S. Dungey, D. Lewis, D.E. Williams, I.P. Parkin, J. Electrochem. Soc. 156 (2009) J46–J51.
[82] K. Sahner, D. Schönauer, M. Matam, M. Post, R. Moos, Sens. Actuators, B: Chem. 130 (2008) 470–476.
[83] K. Sahner, D. Schönauer, P. Kuchinke, R. Moos, Sens. Actuators, B: Chem. 133 (2008) 502–508.
[84] Y.Y. Fong, A.Z. Abdullah, A.L. Ahmad, S. Bhati, Sens. Lett. 5 (2007) 485–499.
[85] M. Vilaseca, J. Coronas, A. Cirera, A. Cornet, J. Morante, J. Santamaría, Catal. Today 82 (2003) 179–185.
[86] M. Vilaseca, J. Coronas, A. Cirera, A. Cornet, J.R. Morante, J. Santamaria, Sens. Actuators, B: Chem. 124 (2007) 99–110.
[87] M. Vilaseca, J. Coronas, A. Cirera, A. Cornet, J. Morante, J. Santamaria, Sens. Actuators, B: Chem. 133 (2008) 435–441.
[88] U. Simon, M.E. Franke, Microporous Mesoporous Mater. 41 (2000) 1–36.
[89] T. Sancho, J. Lemus, M. Urbitzondo, J. Soler, M.P. Pina, Microporous Mesoporous Mater. 115 (2008) 206–213.
[90] W. Mortier, R. Schoonheydt, Prog. Solid State Chem. 16 (1985) 1–125.
[91] O. Schaf, H. Ghobarkar, F. Adolf, F.P. Knauth, Solid State Ionics 143 (2001) 433–444.
[92] O. Schäf, V. Wernert, H. Ghobarkar, P. Knauth, J. Electroceram. 16 (2006) 93–98.
[93] M. Urbitzondo, S. Irusta, R. Mallada, M.P. Pina, J. Santamaría, Desalination 200 (2006) 601–603.
[94] R. Moos, R. Müller, C. Plog, A. Knezevic, H. Leye, E. Irion, T. Braun, K. Marquardt, K. Binder, Sens. Actuators, B Chem. 83 (2002) 181–189.
[95] M. Franke, U. Simon, R. Moos, A. Knezevic, R. Müller, C. Plog, Phys. Chem. Chem. Phys. 5 (2003) 5195–5198.
[96] G. Hagen, A. Dubbe, F. Rettig, A. Jerger, T. Birkhofer, R. Müller, C. Plog, R. Moos, Sens. Actuators, B Chem. 119 (2006) 441–448.
[97] R. Moos, K. Sahner, G. Hagen, A. Dubbe, Rare Met. Mat. Eng. 35 (2006) 447–451.
[98] R. Moos, K. Sahner, M. Fleischer, U. Guth, N. Barsan, U. Weimar, Sensors 9 (2009) 4323–4365.
[99] R. Moos, D. Schönauer, Sens. Lett. 6 (2008) 821–825.
[100] R. Moos, Sensors 10 (2010) 6773–6787.
[101] D. Schönauer, K. Wiesner, M. Fleischer, R. Moos, Sens. Actuators, B Chem. 140 (2009) 585–590.
[102] G. Hagen, A. Schulz, M. Knörr, R. Moos, Sensors 7 (2007) 2681–2692.
[103] A. Fischerauer, A. Gollwitzer, F. Thalmayr, G. Hagen, R. Moos, G. Fischerauer, Sens. Lett. 6 (2008) 1019–1022.
[104] A. Zampieri, A. Dubbe, W. Schwieger, A. Avhale, R. Moos, Microp. Mesop. Mater. 111 (2008) 530–535.
[105] X.G. Li, P.K. Dutta, J. Phys. Chem. C 114 (2010) 7986–7994.
[106] S. Neumeier, T. Echterhof, R. Bölling, H. Pfeifer, U. Simon, Sens. Actuators, B Chem. 134 (2008) 171–174.
[107] T. Bein, K.D. Brown, G.C. Frye, C.J. Brinker, U.S. Patent 5151,110, September 21, 1992.
[108] Y. Yan, T. Bein, Chem. Mater. 4 (1992) 975–977.
[109] S. Mintova, T. Bein, Microporous Mesoporous Mater. 50 (2001) 159–166.
[110] M. Osada, I. Sasaki, M. Nishioka, M. Sadakata, T. Okubo, Microp. Mesop. Mater. 23 (1998) 287–294.
[111] I. Sasaki, H. Tsuchiya, M. Nishioka, M. Sadakata, T. Okubo, Sens. Actuators, B 86 (2002) 26–33.
[112] M. Vilaseca, C. Yagüe, J. Coronas, J. Santamaría, Sens. Actuators, B 117 (2006) 143–150.
[113] C.A. Grimes, C.S. Mungle, K. Zeng, M.K. Jain, W.R. Dreschel, M. Paulose, K.G. Ong, Sensors 2 (2002) 294–313.
[114] C.A.Grimes, P.G. Stoyanov, U.S. Patent 6397,661, June 4, 2002.
[115] I.G. Giannakopoulos, D. Kouzoudis, C.A. Grimes, V. Nikolakis, Adv. Funct. Mater. 15 (2005) 1165–1170.
[116] L. Gora, J. Kuhn, T. Baimpos, V. Nikolakis, F. Kapteijn, E.M. Serwicka, Analyst 134 (2009) 2118–2122.
[117] L. Scandella, G. Binder, T. Mezzacasa, J. Gobrecht, R. Berber, H.P. Lang, C.H. Gerber, J.K. Gimsewski, J.H. Koegler, J.C. Hansen, Microporous Mesoporous Mater. 21 (1998) 403–409.
[118] R. Berger, Ch. Gerber, H.P. Lang, J.K. Gimzewski, Microelectr. Eng. 35 (1997) 373–379.
[119] J. Zhou, P. Li, S. Zhang, Y.P. Huang, P.Y. Yang, M.H. Bao, G. Ruan, Microelectr. Eng. 69 (2003) 37–46.
[120] J. Zhou, P. Li, S. Zhang, Y.C. Long, F. Zhou, Y.P. Huang, P.Y. Yang, M.H. Bao, Sens. Actuators, B-Chem 94 (2003) 337–342.
[121] T. Wakayama, T. Kobayashi, N. Iwata, Sens. Actuators, A Phys 126 (2006) 159–164.
[122] M.A. Urbiztondo, I. Pellejero, M. Villarroya, J. Sesé, M.P. Pina, I. Dufour, J. Santamaría, Sens. Actuators, B 137 (2009) 608–616.
[123] I. Pellejero, M.A. Urbiztondo, M. Villarroya, J. Sesé, M.P. Pina, J. Santamaría, Microporous Mesoporous Mater. 114 (2008) 110–120.
[124] J. Agusti, I. Pellejero, G. Abadal, G. Murillo, M.A. Urbiztondo, J. Sesé, M. Villarroya-Gaudó, M. Pina, J. Santamaría, N. Barniol, Microelectr. Eng. 87 (2010) 1207–1209.